Current Status and Future Trends of Photonic-Integrated FBG Interrogators

Yisbel Eloisa Marin, Tiziano Nannipieri, Claudio J. Oton, and Fabrizio Di Pasquale

***Abstract*—In this paper, we present an overview of the current efforts toward integration on chip of fiber Bragg grating (FBG) sensor interrogators. Different photonic-integration platforms are discussed, including monolithic planar lightwave circuit technology, silicon on insulator (SOI), indium phosphide, and gallium arsenide material platforms. Furthermore, various possible techniques for wavelength metering and methods for FBG multiplexing are discussed and compared in terms of resolution, dynamic performance, multiplexing capabilities, and reliability. The use of linear filters, array waveguide gratings (AWG) as multiple linear filters, and AWG-based centroid signal processing techniques are presented as well as interrogation techniques based on tunable microring resonators and Mach–Zehnder interferometers for phase sensitive detection. FBG sensor interrogation based on SOI platform using active and passive phase sensitive detection is also described, demonstrating specifically the potential of passive phase demodulation for high-speed dynamic strain measurements. This paper finally presents the challenges and perspectives of photonic integration to address the increasing requirements of several industrial applications.**

***Index Terms*—Fiber Bragg gratings, fiber sensors, glass waveguides, high-volume manufacturing services, semiconductors, silicon on insulator, waveguides, wavelength division multiplexing, wavelength meters.**

I. Introduction

FIBER Bragg grating (FBG) sensors have been investigated for several decades and applied as monitoring solutions in a wide range of industrial fields, ranging from transportation to structural health monitoring (SHM), from energy production to oil and gas [1]. Their compactness, light weight, immunity to electromagnetic interference, and resistance to harsh environments make them attractive compared to conventional electrical sensors. Additionally, the use of multiplexing techniques, such as time and wavelength-division multiplexing (WDM), allows for quasi-distributed sensing along a single optical fiber. The sensor system also requires the use of a readout unit able to remotely interrogate several multiplexed FBGs with high sensitivity, speed and reliability and which should also be suitable to address applications where size, weight and power consumption are critical for operation.

Recent advances in photonic integration are attracting a great deal of attention for the development of such low-cost miniaturized FBG readout units with unprecedented performance in terms of size, weight, reliability, repeatability, power consumption, thermal and vibration stability. In particular, these features can address the increasing high-volume requirements of several terrestrial market sectors, like energy production, transportation and SHM in general, as well as the challenging demand of space applications in terms of robustness, weight and low power consumption.

Photonic Integrated Circuits (PIC) can be fabricated on different material platforms, with their own advantages and limitations, depending on the functions to be integrated. Silica based planar lightwave circuits (PLC) [2] are attractive for passive components like AWGs, thanks to the very low loss of their large-size waveguides, but it is challenging to integrate active components due to process incompatibilities with other platforms. In this regard, III-V-material-based photonic platforms such as InP or GaAs [3] have desirable properties for direct integration of active components like sources and detectors, however due to their higher loss they are not typically used for passive devices. On the other hand, the Silicon-on-Insulator (SOI) platform [4] with a very high refractive index contrast, allows the realization of high-density PICs exploiting complementary metal–oxide–semiconductor (CMOS) compatible processes, which potentially allows the combination of both photonic and electronic functionalities into the same chip [5]. A great variety of passive and active devices have been demonstrated in SOI, such as AWGs, modulators and filters, however, silicon lacks the capability of lasing or detecting light at the telecom wavelengths. Many efforts have been focused on integrating photodetectors in SOI either by hybrid integration of III-V components or by direct growth of germanium photodiodes [5], therefore this platform seems to provide all the elements for the design of cost-effective dynamic interrogation units, except for the source which can be coupled off-chip. Comparing cost and performance provided by the different technology platforms, silicon based devices seem to be the most attractive solution. Note that for each technology platform special attention must be paid to packaging issues which play a key role to ensure reliable optical and electrical interconnection of the chip to the external world at low cost.

The potential of PIC technology to replace traditional assembly of multiple discrete optoelectronic components by a single

Manuscript received July 27, 2017; revised November 4, 2017; accepted November 23, 2017. Date of publication December 3, 2017; date of current version February 24, 2018. *(Corresponding author: Yisbel Eloisa Marin.)*

The authors are with the Scuola Superiore Sant'Anna, Institute of Communication, Information and Perception Technologies, Pisa 56124, Italy (e-mail: y.marin@sssup.it; t.nannipieri@sssup.it; claudio.oton@santannapisa.it; f.dipasquale@sssup.it).

Color versions of one or more of the figures in this paper are available online at http://ieeexplore.ieee.org.

Digital Object Identifier 10.1109/JLT.2017.2779848

TABLE I
PERFORMANCE COMPARISON OF THE DIFFERENT FBG INTEGRATED READOUT UNITS TECHNOLOGIES

Technique	Dynamic Range	Sampling Frequency	Optical Output Power	Wavelength Resolution	Multiplexing capacity
WDM with dispersion filter or AWG. [2]	≤10000 με (1 FBG) ≤2500 με (12 FBGs)	2 kHz (1 FBG) 20 kHz (5 FBG)	< 5 dBm	± 5 pm @ 100 Hz	Dispersion Filter: <12 FBG. AWG: >12
Spectrometry: High crosstalk AWG. [3] [10]	4000 με /4.8 nm (8 FBGs)	19.2 kHz	External: 5mW (>90% reflectivity FBGs)	5 pm	1 Sensing Channel: up to 8 FBG
Microring resonator. [11]	1600 με (1 FBG)	Only static results	Not specified	49 pm	Potentially WDM or TDM.
Spectrometry: High crosstalk AWG/ hybrid integration. [9]	5°C and 80°C (4 FBGs)	2 kHz	0.8 mW (−1 dBm)	± 10 pm	WDM: 4 FBGs using an 8-channel AWG.
Active phase demodulation (MZI) [7]	Single FBG: FBG range-limited AWG: Channel space-limited	100 kS/s	External BBS: 27 dBm (10% reflectivity FBGs)	1.99 pm	WDM: 16 FBG with external 16-channel AWG.
Pasive phase demodulation (MZI) [8]	Single FBG: FBG range-limited. AWG: Channel space-limited	100 kS/s	External BBS: 27 dBm (10% reflectivity FBG); 12 dBm (85% reflectivity FBG)	10% reflectivity: 2.5 pm 85% reflectivity: 0.873pm	Potentially WDM or TDM.

small form factor chip opens the way to the development of integrated sensor readout units, which are extremely attractive for future optical sensor systems.

In this paper, after a first overview of recent advances in photonic integration for FBG readout units development [6], we will describe SOI based active and passive FBG phase demodulation techniques [4], [7], [8], based on unbalanced MZIs. The proposed schemes allow in principle the integration of both photonic and electronic required functionalities, excluding the light source, allowing for fast and accurate dynamic interrogation of a large number of FBG sensors. In particular, after briefly summarizing our recent results concerning SOI active phase generated carrier demodulation techniques [7], we experimentally demonstrate fast dynamic interrogation of FBG sensors using an integrated version of the passive scheme described in [9]. Finally, we address the challenges and perspectives for integrated FBG readout units on chip and the conclusions.

II. OVERVIEW ON FBG SENSORS INTERROGATORS ON CHIP

Recently, several efforts towards the photonic integration of FBG sensor readout units have been presented, based on silica glass, InP and SOI material platforms, as summarized in Table I. In [2] an FBG sensor interrogation system based on a dispersive filter was realized on a PLC. This technology allows the hybrid monolithic integration of both active and passive devices by using a silicon substrate as an optical bench, which in turn is mounted on a CMOS electronic board where the processing takes place, resulting in a packaged device with dimensions ranging from 18.5 mm × 18.5 mm × 50 mm to 29 mm × 29 mm × 110 mm, depending on the number of sensing channels. The principle of operation of the readout unit is based on a passive demodulation technique, which exploits WDM filtering through either a selective dispersive filter, for reading less than 12 channels, or an array waveguide grating (AWG), for reading more than 12 channels. The spectral characteristics of the filters are selected such that it is possible to convert the Bragg Wavelength shift into a linear intensity variation, allowing the extraction of the peak wavelength position at the photodetector. The system provides high speed dynamic interrogation, with sampling rate up to 20 kHz, but the technology is limited in terms of active function integration and multiplexing capabilities, with a strain range of $\leq 10000\,\mu\varepsilon$ for 1 sensing channel and $\leq 2500\,\mu\varepsilon$ for 12 channels. In [3] a specially designed AWG, characterized by high crosstalk among its channels, has been realized on InP platform and used as a spectrometer to interrogate wavelength multiplexed FBG sensors. This AWG has a photodetector at each output and the power distribution of the spectral overlap between the FBG and the AWG channels transmittance allows to extract the wavelength shift; the device is however characterized by limited multiplexing capabilities, since it requires multiple AWG channels to interrogate each FBG, hence there is a trade-off between the number of FBGs that can be read and the wavelength dynamic range. The device is capable to interrogate up to 8 FBG sensors, characterized by a $>90\%$ reflectivity, with a dynamic range of $4000\,\mu\varepsilon$ and a sampling frequency of 19.2 kHz [10]. On the other hand, a SOI based micro-ring resonator (MRR) has been used in [11] as a tunable filter for FBG interrogation. The device exploits the large thermo-optic effect in Si to tune and detune the MRR in order to follow the shifts in the Bragg wavelength of the FBG. In order to do this, a periodic signal is applied to micro-heaters placed on top of the MRR. The time domain signal resulting from the scanning can be used to determine the wavelength shift; the proposed technique allows high integration but it is also affected by a dynamic performance and multiplexing capabilities trade-off, with a dynamic range of $1600\,\mu\varepsilon$, limited by double resonance peaks of the micro-ring resonator. A different interrogation system on SOI platform based on a 1×8 AWG was proposed in [12]. The device integrates all the optical components, including an InP-based vertical-cavity surface-emitting laser (VCSEL) and InGaAs-based photodetectors both integrated on top of the SOI chip using hybrid integration. The light from the VCSEL is coupled to the circuit using grating couplers. The principle of operation of the readout unit consists in placing the central FBG wavelength in the middle of the central wavelengths of two adjacent AWG channels, then if there is a shift in the Bragg wavelength the power distribution in each

of the adjacent channels will change, allowing to demodulate the FBG. This device is capable of simultaneously interrogating up to 4 FBGs, with a sampling frequency of 2 kHz, with its multiplexing capabilities limited by the number of channels and channel spacing of the AWG, since each FBG requires two channels for interrogation.

Comparing the different technologies so far (see Table I) it is clear that spectrometry and dispersive filter based readout units [2], [3], [10] provide a good wavelength resolution, suitable for static measurements, where stability and accuracy are required, and could also be used for dynamic measurements but not at very high frequencies, which is necessary for monitoring vibrations. For the MRR and hybrid integration based techniques only static measurements are demonstrated, but the performance is not as good as the reported in [2], [3], [10]. In the following chapters we will address two different approaches based on unbalanced MZI that provide a better wavelength resolution with a good dynamic range and dynamic strain resolution, one of which is capable of measuring high frequency vibrations.

III. SOI-Based Active Phase Demodulation Technique

Unbalanced MZI demodulators can be used to convert FBG sensors Bragg wavelength shift into phase variations of the output signal at the photodetector, allowing for very high resolution interrogation [13]. This type of MZIs is characterized by a differential length *d* between its arms. The spectral period of the fringe pattern is called the free spectral range (FSR) of the MZI. If the spectral width of the FBG is narrower than half the FSR of the MZI, an interference between these signals will be obtained at the output. This output signal can be written as:

$$I = A + B\cos\Delta\varphi(\mathrm{t}), \tag{1}$$

where *A* is the DC component, *B* is proportional to the input intensity and depends on the mixing efficiency of the MZI, and $\Delta\varphi(t)$ is the phase difference between the signals in each arm of the MZI.

However, it is not straightforward to extract the precise phase condition only from the intensity of the output *I*, because the *arc cos* function has two solutions, and its responsivity varies along the fringe position. Active phase demodulation schemes like the phase generated carrier (PGC) technique allow a precise estimation of the phase variations of the signal of interest by applying an external phase modulation on one of the MZI arms, with a frequency much higher than that of the signal of interest [14]. Considering a sinusoidal modulating signal with frequency ω_0 and amplitude *C*, the output (1) of the MZI becomes:

$$I = A + B\cos\left[C\cos\left(\omega_0 t\right) + \Delta\varphi(t)\right]. \tag{2}$$

Eq. (2) can be expanded in terms of Bessel functions and, as reported in detail in reference [7], by mixing the output of the MZI with the proper even and odd multiple of ω_0 and by applying a low-pass filter to the signals to remove the frequencies above the band of interest, it is possible to obtain signals that are proportional to $\sin\Delta\varphi(t)$ and $\cos\Delta\varphi(t)$, from which the phase variations can be extracted by using, for example, the arc-tangent demodulation technique [7].

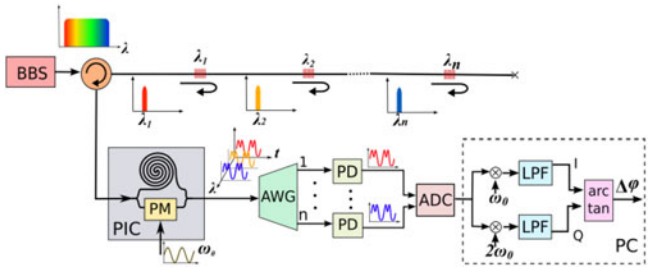

Fig. 1. Schematic of the interrogation system using PGC with WDM. BBS: Broadband Source; PZT: Piezo-Electric Actuator; PIC: Photonic Integrated Circuit; PM: Phase Modulator; PD: Photodetector; ADC: Analog-to-Digital Converter; LPF: Low-Pass Filter; PC: Personal Computer.

Considering mixing signals at ω_0 and $2\omega_0$, it is possible to obtain two signals $\mathrm{S_1}$ and $\mathrm{S_2}$ that are proportional to $\sin\Delta\varphi(t)$ and $\cos\Delta\varphi(t)$ respectively, from which the phase shift can be obtained as $\Delta\varphi(\mathrm{t}) = \arctan(\mathrm{S_2}/\mathrm{S_1})$ and finally, this phase change can be converted into wavelength shift $\Delta\lambda$ relative to the MZI free spectral range $\Delta\lambda_{\mathrm{FSR}}$, using the relation:

$$\Delta\lambda = \frac{\Delta\lambda_{\mathrm{FSR}}\Delta\varphi(t)}{2\pi}. \tag{3}$$

Note that the same MZI can be used to monitor many different FBGs simply by wavelength demultiplexing (WDM) its output using for example an AWG, as depicted in Fig. 1 [7]. This means that only one modulator is needed to track the wavelength of many different gratings simultaneously. Under this configuration, only one channel of the AWG is required to interrogate a single FBG, but multiple channels could be assigned to the same FBG to increase the dynamic range.

IV. SOI-Based Passive Phase Demodulation Technique

In [8] an FBG sensor interrogator in SOI platform based on passive phase demodulation was demonstrated. This approach allows to perform high frequency dynamic detection, since the measurements are not limited by the speed response of the active control. The device consists of an unbalanced MZI with a 3×3 MMI coupler at the output, as shown in Fig. 1, which converts the Bragg wavelength shift into a phase variation of the signals at each output. When the path difference of the MZI is within the coherence length of the light reflected by the FBG, the signal at each output can be written as:

$$V_n = a_n + b_n\cos(\Delta\varphi(t) + \theta_n), \qquad n \in \{1, 2, 3\} \tag{4}$$

where a_{n}, b_{n} and θ_{n} are constants that depend on the Bragg reflection intensity, interferometer modulation depth, and the coupling coefficients of the 3×3 coupler, respectively, and $\Delta\varphi(\mathrm{t})$ is the signal of interest. For a perfect coupler, $\mathrm{a_n}$ and $\mathrm{b_n}$ should be equal, and θ_{n} should be 120° ($\theta_n = 2(n-1)\pi/3$) for $\mathrm{n} \in 1, 2, 3$; however, due to fabrication errors, real couplers can have asymmetric properties that cause deviations of these values from the ideal case. In order to accurately measure the wavelength shifts it is necessary to perform a calibration to determine the current value of the constants. This process consists in applying a phase modulating signal on one of the arms of the MZI to produce a 2π rad peak-to-peak sweep in the transfer

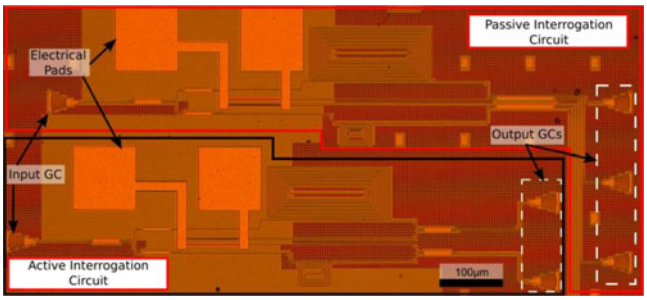

Fig. 2. Optical microscope image of the fabricated devices. The total footprint is 1000 μm × 300 μm. Only the coarse MZI at the bottom of the active and passive was used in this work. GC: Grating coupler.

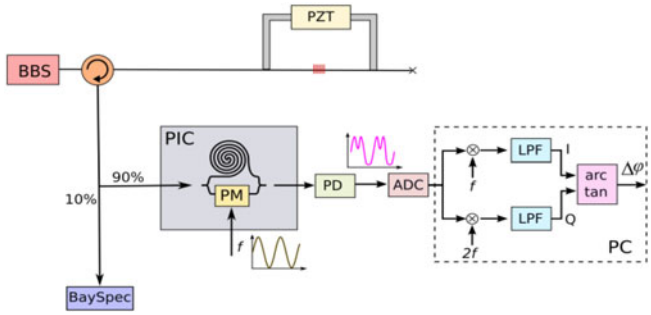

Fig. 3. Experimental Setup. BBS: Broadband Source; PZT: Piezo-Electric Actuator; PIC: Photonic Integrated Circuit; PM: Phase Modulator; PD: Photodetector; ADC: Analog-to-Digital Converter; LPF: Low-Pass Filter; PC: Personal Computer.

function of the MZI [15], which allows to find the output coefficients as $a_n = (V_{n,\max} + V_{n,\min})/2$ and $b_n = (V_{n,\max} - V_{n,\min})/2$. To determine θ_n it is necessary to add the output signals after applying the modulation, obtaining:

$$V_k + V_l = V_{k+l} = a_{k+l} + b_{k+l}\cos\left(\varphi(t) + \theta_{k+l}\right) \quad k \neq l \in 1,2,3 \tag{5}$$

Then, by the law of cosines, it is possible to determine the phase difference between the outputs as:

$$\theta_n = \cos^{-1}\left(\frac{b_{k+l}^2 - b_k^2 - b_l^2}{2b_k b_l}\right) k \neq l \in 1,2,3,\ n \in 1,2,3 \tag{6}$$

By defining the normalizing parameters: $\alpha_n = a_n\ /a_1$, $\gamma_n = b_n\ \sin\theta_n/(b_1\alpha_n)$, $\mu_n = b_n\ \cos\theta_n/(b_1\alpha_n)$, and defining $\overline{V_2} = V_2\ /\alpha_n$ and $\overline{V_3} = V_3\ /\alpha_3$ the signal of interest can be expressed $\varphi(t)$ as:

$$\varphi(t) = \tan^{-1}\left(\frac{(\mu_2 - \mu_3)V_1 + (\mu_3 - \mu_1)\bar{V}_2 + (\mu_1 - \mu_2)\bar{V}_3}{(\gamma_2 - \gamma_3)V_1 + (\gamma_3 - \gamma_1)\bar{V}_2 + (\gamma_1 - \gamma_2)\bar{V}_3}\right) \tag{7}$$

Finally, the phase shift $\Delta\varphi(t)$ can be converted into the corresponding FBG wavelength shift $\Delta\lambda$ using (3).

The regularity of the calibration will depend on the stability of the design. Some approaches that could potentially reduce or eliminate the need for a periodic calibration are: using a precise temperature control, implementing an athermal MZI design [16], and integrating the photodiodes in the circuit, as demonstrated on a SOI platform in [4].

V. Design and Fabrication of the Devices

The devices (see Fig. 2) were fabricated from 8" SOI wafers with 220 nm silicon thickness and 2 μm buried oxide. Deep-UV 193 nm optical lithography was used to pattern 220 nm × 48 nm single-mode waveguides. Focusing grating couplers were used for vertically coupling the light from single-mode fibers at 11°. A coupling loss of ~5.5 dB per grating was measured from a reference sample. The photonic circuit includes two MZIs, one with path difference $\Delta L = 5000\,\mu$m (so-called fine), and another one with $\Delta L = 500\,\mu$m (so-called coarse), generating fringe patterns with FSRs of 0.11 nm and 1.1 nm respectively. The longer branches were spiraled to minimize footprint, resulting in a total circuit footprint of 1000 μm × 300 μm. Additionally, the short branch of both MZIs includes a thermal phase modulator, which consists of a metal Ti/TiN heater track which is 86 μm long and 1.4 μm wide. This modulator has a 1/e time-constant of 7 μs and a $V_{2\pi}$ of 3.6 V. Note that since the FBGs used are characterized by a full width at half maximum (FWHM) bandwidth of ~ 80 pm, and ~250 pm in case of fast dynamic passive phase demodulation measurements, only the coarse MZI (with FSR 1.1 nm) could be used, as the FSR of the fine is too small (0.11 nm).

VI. Experimental Results

A. Experimental Setup and Results for PGC Demodulation Technique

The experimental setup used for the dynamic characterization of the FBGs based on PGC demodulation is shown in Fig. 3; the output of a wideband light source from BaySpec Inc. (centered at 1550 nm with a spectral width of 100 nm) was amplified using a high power EDFA and then coupled to the FBG under test using a three-port optical circulator (OC). The FBG from FBGS Technologies GmbH, characterized by a Bragg wavelength of ~1558 nm, a full width at half maximum (FWHM) bandwidth of ~ 80 pm, and a reflectivity of 10%, was longitudinally strained using a piezo-electric actuator (PZT). The FBG was actually pre-strained using a micrometer, in order to apply dynamic strain effectively, thus increasing the grating compression sensitivity. The reflection from the FBGs is divided using a 90/10 coupler; the 10% of the signal is sent to a commercial readout unit from Bayspec Inc., while the 90% part is coupled to the device under test. The comparison of the results under this uneven splitting condition is fair since the spectrometer-based Bayspec provides the central wavelength of the FBG using a detection threshold defined above the background noise, so increasing the power would not improve the SNR. The PIC output is then coupled to an InGaAs based photoreceiver with a trans-impedance amplifier and 12 kHz bandwidth. Finally, the photoreceiver electrical signal is connected to a DAQ (100 kS/s) for data acquisition and processing on a PC.

A sinusoidal signal of 275 Hz of frequency and 1.2 V peak-to-peak with 1 V DC component was applied to the PZT driver in order to strain the FBG. Simultaneously, the thermal phase modulator in one of the arms of the MZI was driven using

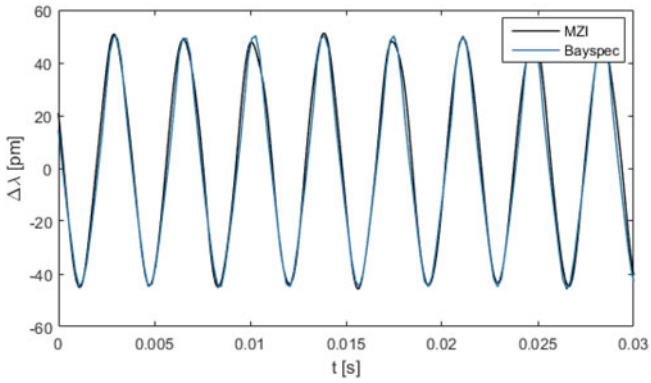

Fig. 4. Comparison of the measured wavelength shift versus time obtained with the device under test (in black) and the commercial FBG readout from BaySpec Inc. (in blue).

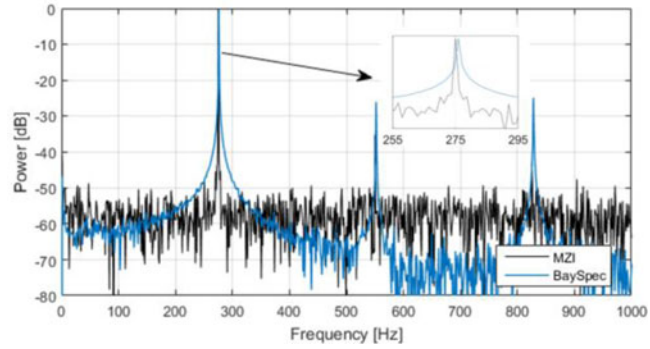

Fig. 5. Comparison of the spectra of the measured wavelength variation signals with the MZI and BaySpec Inc. readout unit.

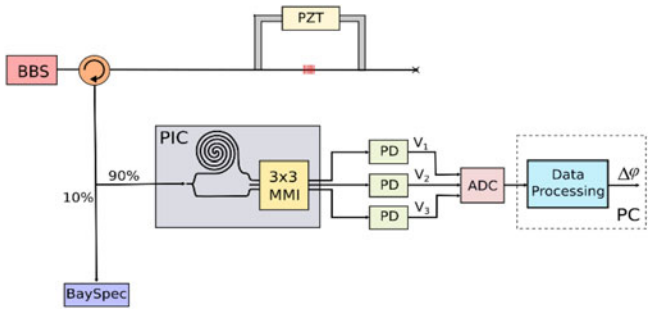

Fig. 6. Experimental Setup. BBS: Broadband Source; PZT: Piezo-Electric Actuator; PIC: Photonic Integrated Circuit; PD: Photodetector; ADC: Analog-to-Digital Converter; PC: Personal Computer.

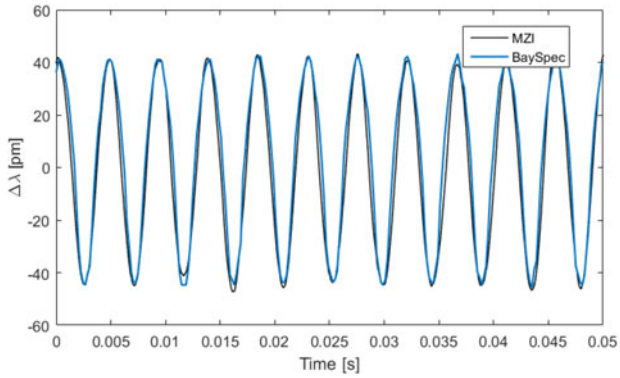

Fig. 7. Comparison of the measured wavelength shift versus time obtained with the device under test (in black) and the commercial FBG readout from BaySpec Inc. (in blue).

the square-root of a sinusoidal signal, since the applied power is proportional to the square of the voltage. The peak-to-peak amplitude was 3.3 V and the frequency was 5 kHz, which is more than ten times the frequency of variation of the Bragg wavelength.

Fig. 4 compares the estimated wavelength shift obtained by applying the PGC demodulation technique and the commercial FBG readout unit from BaySpec Inc. Note that the integrated device accurately measures variations of approximately 97 pm peak-to-peak, presenting a good agreement with the commercial readout unit results.

The spectra of the measured wavelength shift signals, normalized to the peak power of the BaySpec signal, are shown in Fig. 5. The higher spectral width of the BaySpec signal with respect to the MZI signal could be due to lack of precision of the timestamp generated with the data of the readout unit, which could also justify the fact that the frequency peak is located slightly above 275 Hz. A signal-to-noise ratio (SNR) normalized to a 1-Hz bandwidth of approximately 51.9 dB was measured for the MZI, whereas for the BaySpec was approximately 69.9 dB, which results in a dynamic strain resolution of 72.3 $n\varepsilon/\sqrt{Hz}$ and 9 $n\varepsilon/\sqrt{Hz}$ respectively. The PIC performance can be improved by reducing the total circuit loss and by integrating the photoreceivers in the same chip. Comparing the performance of this device with the ones previously reviewed in Section II, the unbalanced MZI with active interrogation shows a better wavelength precision, while having a very good dynamic resolution and dynamic range. In terms of multiplexing capabilities, the number of FBGs that can be interrogated by a single device will depend on the number of channels of the AWG, being possible to dedicate more than one channel per FBG to increase the dynamic range

B. Experimental Setup and Results for Passive Demodulation Technique

The experimental setup used for the dynamic characterization of the FBGs based on the passive phase demodulation technique is reported in Fig. 6. The amplified spontaneous emission (ASE) from a high power EDFA is used as a broad band source and coupled to the FBG fiber under test using a three-port optical circulator (OC).

The PIC performance has been first evaluated by applying longitudinal dynamic strain on the pre-strained FBG from FBGS Technologies GmbH, characterized by a FWHM bandwidth of $\sim$80 pm, a Bragg wavelength of $\sim$1558 nm and $\sim$10% reflectivity, and comparing the measurement with a commercial readout unit from Bayspec Inc.. The calibration procedure has been implemented by controlling a thermal modulator with the square-root of a sinusoidal signal with amplitude $V = 4.25\,V$ and frequency $f = 500\,Hz$. The signals V1, V2 and V3 recorded at the outputs of the MMI were used to calculate the calibration parameters a_n, b_n and θ_n. The phase differences between ports were found to be 117.15° and 116.63°, instead of the ideal 120°. The results presented in Fig. 7 demonstrate that the device

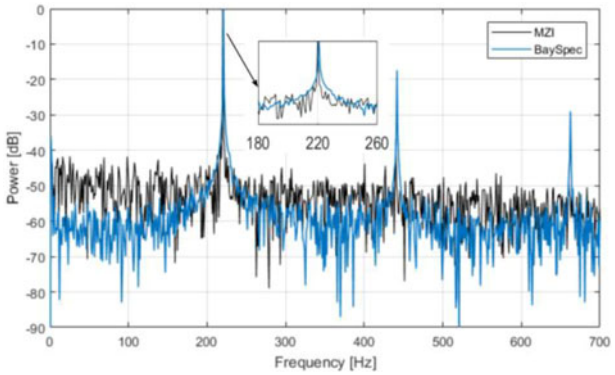

Fig. 8. Comparison of the spectra of the measured wavelength variation signals with the MZI and BaySpec Inc. readout unit.

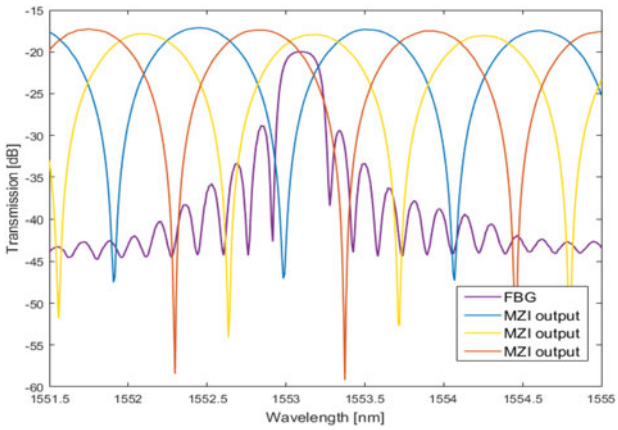

Fig. 9. Measured spectral response of the MZI and comparison with the pre-strained FBG spectral width centered at 1553.1 nm.

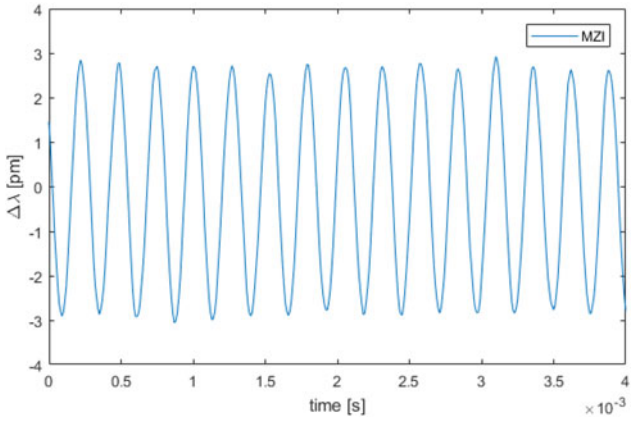

Fig. 10. Wavelength shift versus time obtained with the device under test when applying a 3.82 kHz signal to the piezo speaker driver.

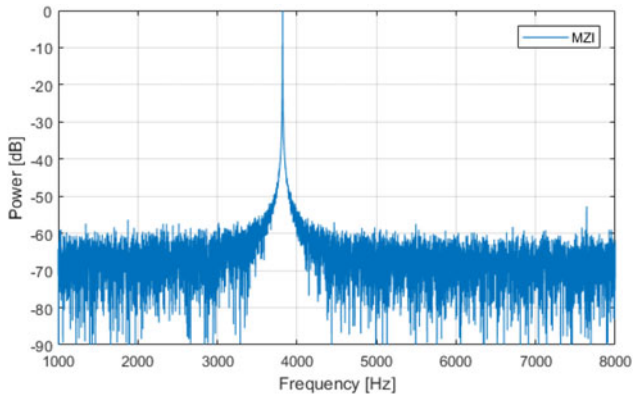

Fig. 11. Spectra of the measured wavelength variation signal obtained with the device under test when applying a 3.82 kHz signal to the piezo speaker driver.

accurately measures wavelength shifts of approximately 90 pm peak-to-peak, showing a good agreement with the commercial readout unit results.

The spectra of the measured wavelength shift signals, normalized to the peak power of the one obtained with the BaySpec, are shown in Fig. 8. The dynamic strain resolution for the Bayspec was of 25 $n\varepsilon/\sqrt{Hz}$ versus 82 $n\varepsilon/\sqrt{Hz}$ for the proposed PIC. Also in this case note that the PIC performance can be improved by reducing the PIC loss and by integrating the photodetectors.

In order to fully demonstrate the dynamic measurement capabilities of the SOI passive phase demodulation technique, further experimental analysis has been carried out; a different FBG from Innovative Fibers Inc., was employed, since the one used in the previous experiment was attach to a different actuator and an identical one was not available at the moment of the experiment. The FBG, characterized by a Bragg wavelength of ∼1552.78 nm, a 3-dB bandwidth of 250 pm and ∼85% reflectivity, was strained by the vibrations generated by a piezo speaker. To achieve this, the fiber was fixed to the surface of the piezo speaker on two longitudinal points around the FBG. The FBG was pre-strained during the gluing, resulting in a Bragg wavelength of 1553.1 nm, as depicted in Fig. 9. The reflection from the FBG was coupled to the device under test and the output ports of the chip processed as already described in Section IV. The calibration steps explained in Section IV were performed before every measurement. This was a precaution since any small change in the alignment of the fiber array used would cause the calibration parameters to change. We believe that by gluing the fiber array to the chip or integrating the photodetectors the frequency of the measurements would be significantly reduced.

First, we applied a signal at 3.82 kHz to the amplifier that drives the piezo speaker, measuring a change in the Bragg wavelength of ∼6 pm peak-to-peak, as shown in Fig. 10. A Savitzky-Golay filter with cut-off frequency of 12.17 kHz was applied to smooth the traces acquired at the output of the MZI before applying the algorithm explained in Section IV, preserving the actual spectral energy of the demodulated signal.

The spectrum of the signal is shown in Fig. 11. A signal-to-noise ratio (SNR) normalized to a 1-Hz bandwidth of ∼64 dB was measured.

Finally, we applied a signal of 7.21 kHz to the amplifier that drives the piezo speaker, measuring a signal of ∼2 pm peak-to-peak, as reported in Fig. 12. Since the wavelength shift produced by the piezo speaker vibrations at this frequency was so small, the signal detected by the photo-receivers presented a high level of noise, therefore a Savitzky-Golay filter with cut-off frequency of 23.34 kHz was applied to smooth the acquired traces before processing.

The spectrum of the signal is shown in Fig. 13. A signal-to-noise ratio (SNR) normalized to a 1-Hz bandwidth of ∼54.3 dB

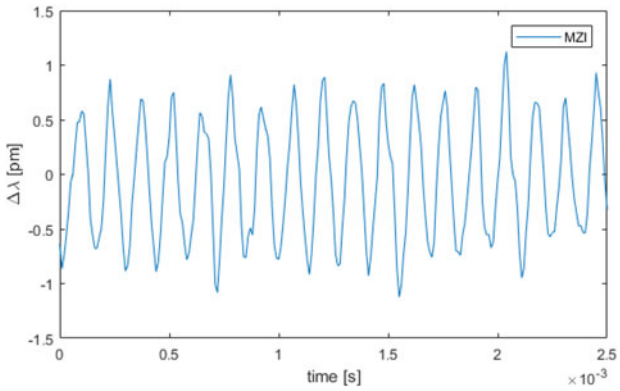

Fig. 12. Wavelength shift versus time obtained with the device under test when applying a 7.21 kHz signal to the piezo speaker driver.

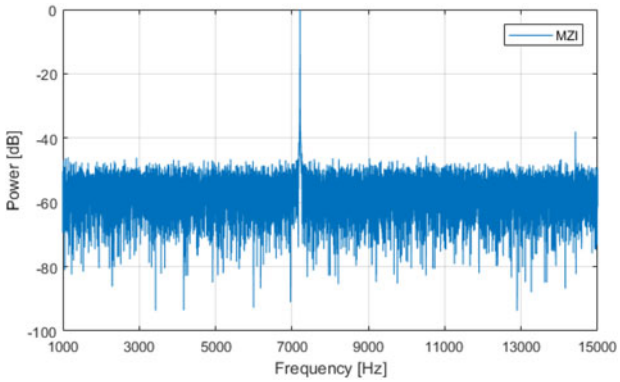

Fig. 13. Spectrum of the measured wavelength variation signals with the MZI corresponding to applied sinusoidal signal at 7210 Hz.

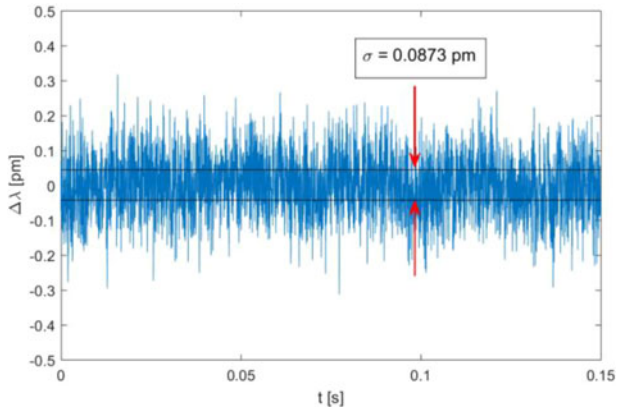

Fig. 14. Minimum detectable wavelength of the device under test in a 10-kHz bandwidth.

was measured. The dynamic strain resolution of the device is $\sim 0.91\, n\varepsilon/\sqrt{\text{Hz}}$.

To determine the minimum detectable wavelength of the PIC, the back-reflected signal from the FBG was recorded without applying any signal to the piezo speaker. Fig. 14 shows the demodulated signal in time domain. A minimum detectable signal, corresponding to the standard deviation of the noise in a 10 kHz bandwidth, of 0.0873 pm was obtained, which shows that the device is capable of measuring small wavelength variations at high speed. These results, summarized in Table I, show that the passive interrogation scheme is suitable for applications that require measuring high frequency vibrations with a very good wavelength resolution, below the typical 1 pm resolution that most commercial devices provide. In fact, the limits of interrogation of this device have not been demonstrated yet, since the maximum frequency of the experiments was constrained by the capabilities of the available piezo actuator.

VII. Challenges and Perspectives

There are still some challenges to be addressed in order to make integrated FBG sensor interrogators really competitive with bulk components based readout units. The integration of the source is still one of the challenges to overcome to achieve a fully integrated readout unit. Two of the main desired requirements for the source are: a good power efficiency to obtain enough output optical power, and integration on SOI through a CMOS-compatible process to allow high production levels and cost effectiveness. Hybrid and heterogeneous integration of III-V sources on SOI have been demonstrated showing high optical output power, however the incompatibility with CMOS makes integration complicated and costly. Other approaches have been proposed such as the use of erbium-doped Si-rich materials, which are CMOS-compatible, but have low power efficiency, and Ge-on-Si based sources, characterized by a large gain spectrum and CMOS compatibility, but have a very high threshold current [17] leading to a potential high-power consumption of the readout unit, which is not desirable for certain applications.

Another important challenges involve the packaging of the readout unit, which on itself represents a big portion of the cost of a functional photonic device. The packaging process includes the alignment of optical fiber to the chip, which is a challenging step due to the mode size mismatch between the integrated waveguides (hundreds of nm) and optical fibers ($\sim 10\ \mu$m for single-mode fibers). The alignment can be accomplished mainly through vertical coupling using grating couplers, with alignment tolerances of $1 - 2\ \mu$m, or through edge-coupling, with sub-micron tolerances. In both cases active alignment is implemented, which is time consuming and involves expensive equipment. Many efforts towards passive alignment are being made, however there is still not a predominant technique that solves all the alignment challenges [18]. Packaging also requires electrical connections and precise temperature control, since silicon photonics components are particularly sensitive to temperature changes. Usually this can be taken care of by using a thermoelectric coolers (TEC), which prices vary according to the precision of the controller. An alternative that would allow to relax the TEC requirements would be the use of athermal designs, which is a topic currently being investigated.

There are also other requirements for packaging related to the external conditions under which the device will operate, such as hermeticity, shock and vibration stability, radiation hardening, and outgassing. We could classify the packages according to the severity of these requirements as: general-application packages, which could be used for readout units without strict requirements, and application-specific packages, with more rigorous requirements. The latter apply particularly to spaceborne devices that must pass strict validation tests and certifications to prove they can resist rough launching conditions and can operate

in harsh environments. Regardless of the case, the ultimate goal is to simplify the packaging process and reduce the cost through standardization of the design rules by implementing packaging design kits (PDKs) and rules (PDR) [18], however, their industry-wide implementation is still in its very early stages.

VIII. Conclusion

In this paper we reviewed different efforts towards the integration of Fiber Bragg Grating (FBG) sensor interrogators. The different measurement approaches and the available technological platforms demonstrate that there is a strong potential for several applications and also justify the interest from both academy and industry in the development of compact and reliable integrated FBG readout units.

Comparing cost and performance provided by the different technology platforms, silicon based devices seem to be the most attractive solution in many situations, especially in high-volume applications. For this reason, we have specifically reported experimental results concerning FBG sensor interrogation based on SOI platform using active and passive phase sensitive detections. Particularly, we demonstrated high speed measurements of up to 7.21 kHz using the passive demodulation technique, with a dynamic strain resolution of 0.91 $n\varepsilon/\sqrt{\text{Hz}}$ and a minimum detectable wavelength shift of 0.0873 pm.

References

[1] B. Culshaw and A. Kersey, "Fiber-optic sensing: A historical perspective," *J. Lightw. Technol.*, vol. 26, no. 9, pp. 1064–1078, May 2008.

[2] E. Mendoza *et al.*, "Fully integrated miniature multi-point fiber Bragg grating sensor interrogator (FBG-transceiver^{TM}) system for applications where size, weight, and power are critical for operation," in *Proc. 6th Eur. Workshop Struct. Health Monitoring*, Dresden, Germany, 2012, pp. 1–7.

[3] R. Evenblij and J. Leijtens, "Space gator: A giant leap for fiber optic sensing," in *ICSO Spain Int. Conf. Space Opt.*, Tenerife Spain, 2014. [Online]. Available: http://www.icsoproceedings.org/. Accessed on: Aug. 12, 2017.

[4] A. Ruocco and W. Bogaerts, "Fully integrated SOI wavelength meter based on phase shift technique," in *Proc. IEEE 12th Int. Conf. Group IV Photon.*, Vancouver, BC, Australia, 2015, pp. 131–132.

[5] L. C. Kimerling *et al.*, "Electronic-photonic integrated circuits on the CMOS platform," *Proc. SPIE*, vol. 6125, 2006, Art. no. 612502.

[6] Y. Marin *et al.*, "Fiber Bragg grating sensor interrogators on chip: Challenges and opportunities," *Proc. SPIE*, vol. 10323, 2017, Art. no. 103230D.

[7] Y. Marin *et al.*, "Integrated FBG sensors interrogation using active phase demodulation on a silicon photonic platform," *J. Lightw. Technol.*, vol. 35, no. 6, pp. 3374–3379, Aug. 2017.

[8] Y. Marin *et al.*, "Integrated FBG sensor interrogator in SOI platform using passive phase demodulation," presented at the Front. Opt. Conf., Rochester, NY, USA, 2016, Paper FF3B.2.

[9] A. D. Kersey *et al.*, "High-resolution fibre-grating based strain sensor with interferometric wavelength-shift detection," *Electron. Lett.*, vol. 28, no. 3, pp. 236–238, 1992.

[10] *Extreme Fiber Sensing Product Catalog 2016*, Technobis tft-fos, Alkmaar, The Netherlands, 2016.

[11] G. Vargas, "Fiber Bragg grating interrogation using a micro-ring resonator tunable filter with peak wavelength detection enhancement," *Proc. SPIE*, vols. 9480, 2015, Art. no. 94800P.

[12] H. Li *et al.*, "Chip-scale demonstration of hybrid III–V/silicon photonic integration for an FBG interrogator," *Optica*, vol. 4, no. 7, pp. 692–700, 2017.

[13] B. Lee and Y. Jeong, "Interrogation techniques for FGSs and the theory of fiber gratings," in *Fiber Optic Sensors*, 2nd ed. Boca Raton, FL, USA: CRC Press, 2008.

[14] A. Dandridge, A. B. Tveten, and T. G. Giallorenzi, "Homodyne demodulation scheme for fiber optic sensors using phase generated carrier," *IEEE Trans. Microw. Theory Techn.*, vol. 30, no. 10, pp. 1635–1641, Oct. 1982.

[15] M. Todd, M. Seaver, and E. Bucholtr, "Improved, operationally passive interferometric demodulation method using 3×3 coupler," *Electron. Lett.*, vol. 38, no. 15, pp. 784–786, 2002.

[16] M. Uenuma and T. Moooka, "Temperature-independent silicon waveguide optical filter," *Opt. Lett.*, vol. 34, pp. 599–601, 2009.

[17] Z. Zhou, B. Yin, and J. Michel, "On-chip light sources for silicon photonics," *Light, Sci. Appl.*, vol. 4, p. e358, 2015.

[18] P. O'Brien *et al.*, "Packaging of silicon photonic devices," in *Silicon Photonics III: Systems and Applications*. Berlin, Germany: Springer-Verlag, 2016, pp. 220–232.

Yisbel Eloisa Marin received the B.Sc. degree in electronic engineering from Universidad Nacional Experimental Politecnica "Antonio Jose de Sucre," Barquisimeto, Venezuela, in 2010, and the M.Sc. degree in photonic networks engineering from both Aston University, Birmingham, U.K. and Scuola Superiore Sant'Anna, Pisa, Italy, in 2015. She is currently working toward the Ph.D. degree in emerging digital technologies, photonic technologies curriculum, at the Institute of Information Communication and Perception Technologies, Scuola Superiore Sant'Anna. Her current research interests include optical fiber sensors and photonic-integrated circuits.

Tiziano Nannipieri was born in Pisa, Italy, in 1980. He received the Laurea degree (B.S.) and the Laurea Magistralis degree (M.S.) in telecommunications engineering from the University of Pisa, Pisa, in 2007 and 2008, respectively.

From 2009 to 2010, he was Consorzio Nazionale Interuniversitario per le Telecomunicazioni scholarship student with the National Laboratory of Photonic Networks, Pisa. He is currently within the Optical Fiber Sensors and Integrated Photonics Subsystems Research Area with the Institute of Communication, Information and Perception Technologies, Scuola Superiore Sant'Anna, Pisa. He is the cofounder and R&D Engineer of INFIBRA TECHNOLOGIES, a Scuola Superiore Sant'Anna spin-off company involved in different sectors ranging from oil and gas to transportation with its own advanced fiber optic sensor systems. He is the author and coauthor of more than 20 scientific journals and conference papers in the area of Optical Fiber Sensors. His research interests include fiber optic sensing, especially in design and development of distributed and discrete fiber optic sensor systems for multiparameter physical sensing based on Raman, Brillouin, and Rayleigh scattering, as well as fiber Bragg gratings.

Mr. Nannipieri is a reviewer of the IEEE/OSA Sensors Journal, the *Optics Express,* the *Optics Letters*, and the *Applied Optics*.

Claudio J. Oton received the Ph.D. degree from the University of La Laguna, San Cristóbal de La Laguna, Spain, in 2005. Then, he spent four years with the *Optoelectronics Research Centre*, Southampton, U.K., where he worked on integrated optical amplifiers and lasers on silicon as a Marie Curie Postdoctoral Fellow. In 2009, he joined *Nanophotonics Research Centre*, Universidad Politecnica de Valencia, Spain, where he studied nonlinear silicon photonic devices. Finally, from 2012, he is an Assistant Professor with TeCIP Institute, *Scuola Superiore Sant'Anna*, Pisa, Italy. He is author of more than 60 peer-reviewed scientific papers and several conference contributions, which yield an *h*-index of 22. His current research interests include optical fiber sensors and silicon photonic-integrated devices.

Fabrizio Di Pasquale received the degree in electronic engineering from the University of Bologna, Bologna, Italy, in 1989, and the Ph.D. degree in information technology from the University of Parma, Parma, Italy, in 1993.

From 1993 to 1998, he was with the Department of Electrical and Electronic Engineering, University College London, U.K., as a Research Fellow, working on optical amplifiers, WDM optical communication systems, and liquid crystal displays. After two years with Pirelli Cavi e Sistemi and two years with Cisco Photonics Italy, he moved to Scuola Superiore Sant'Anna, Pisa, Italy, where he is currently a Full Professor of telecommunications. He is the cofounder and President of INFIBRA TECHNOLOGIES, a spin-off company of Scuola Superiore Sant'Anna, developing and marketing advanced fiber optic sensor systems. He has filed 20 international patents and he is the author and coauthor of more than 200 scientific journals and conference papers. His current research interests include optical fiber sensors, silicon photonics, optical amplifiers, WDM transmission systems, and networks.

Dr. Pasquale is on the Board of Reviewers of the IEEE Photonics Technology Letters, the IEEE/OSA Journal of Lightwave Technology, the IEEE Sensors Journal, the *Optics Communications*, the *Optics Express*, and the *Optics Letters*.